

## 3.10. ACCURACY IN RIETVELD QUANTITATIVE PHASE ANALYSIS

**Table 3.10.1**

Cambridge Structural Database (CSD)/Inorganic Crystal Structure Database (ICSD) reference codes for all phases used for Rietveld refinements in this work and the linear absorption coefficients for the wavelengths used

Phase	Chemical formula	CSD/ICSD refcode	$\mu$ (cm <sup>-1</sup> ), Cu $K\alpha_1$ , $\lambda = 1.5406$ Å	$\mu$ (cm <sup>-1</sup> ), Mo $K\alpha_1$ , $\lambda = 0.7093$ Å	$\mu$ (cm <sup>-1</sup> ), $\lambda = 0.7744/0.4959$ Å	Reference
Glucose	C <sub>6</sub> H <sub>12</sub> O <sub>6</sub>	Glucsa10	12	1	1.3/—	Brown & Levy (1979)
Fructose	C <sub>6</sub> H <sub>12</sub> O <sub>6</sub>	Fructo11	12	1	1.3/—	Kanters <i>et al.</i> (1977)
$\alpha$ -Lactose monohydrate	C <sub>12</sub> H <sub>22</sub> O <sub>11</sub> ·H <sub>2</sub> O	Lactos10	12	1	1.3/—	Fries <i>et al.</i> (1971)
Xylose	C <sub>5</sub> H <sub>10</sub> O <sub>5</sub>	Xylose	12	1	1.2/—	Hordvik (1971)
Gypsum	CaSO <sub>4</sub> ·(H <sub>2</sub> O) <sub>2</sub>	151692	141	16	22/—	De la Torre <i>et al.</i> (2004)
Quartz	SiO <sub>2</sub>	41414	92	10	11/2.9	Will <i>et al.</i> (1988)
s-Anhydrite	CaSO <sub>4</sub>	16382	219	24	31/—	Kirfel & Will (1980)
i-Anhydrite	CaSO <sub>4</sub>	79527	219	24	31/—	Bezou <i>et al.</i> (1995)
Zincite	ZnO	65120	285	244	—/89.1	Albertsson <i>et al.</i> (1989)
Calcite	CaCO <sub>3</sub>	80869	194	22	27/7.3	Maslen <i>et al.</i> (1995)
SrSO <sub>4</sub>	SrSO <sub>4</sub>	22322	299	187	40/—	Garske & Peacor (1965)

sample transmission geometry is conceptually similar to that for flat-plate reflection geometry, but the length of the scattered beam path has to be properly defined. The corresponding equation is given in section A5.2.5 of Egami & Billinge (2003).

It must also be noted that Mo radiation has a major drawback when compared with Cu radiation. The  $\lambda^3$  dependence of diffraction intensity favours the use of Cu radiation by a factor of 10.2. Thus, a detector receives approximately ten times as many diffracted X-ray photons with Cu than with Mo (this calculation neglects the different fractions of photons lost in the diffractometer optical paths). This fact can be partially overcome in modern X-ray detectors by increasing the counting time for patterns collected with Mo radiation without reaching prohibitively long times.

As discussed in Chapter 3.9, there are many factors that affect the accuracy and precision of QPA results. It must be recalled that accuracy is the agreement between the analytical result and the true value, and precision is the agreement between results for analyses repeated under the same conditions. Precision may be further divided into repeatability, the agreement between analyses derived from several measurements on the same specimen, and reproducibility, the agreement including re-preparation, re-measurement and data re-analysis of the same sample. Since the largest sources of errors in RQPA are experimental, sample preparation is key, as the reproducibility of peak-intensity measurements is mainly governed by particle statistics (Elton & Salt, 1996). It is generally accepted that the diffraction intensities have to be collected with an accuracy close to  $\pm 1\%$  to obtain patterns that are suitable for good RQPA procedures (Von Dreele & Rodriguez-Carvajal, 2008). Milling the sample to reduce the particle size is an approach that should be exercised with care to avoid peak broadening or amorphization (Buhrke *et al.*, 1998). In order to improve particle statistics, a very common practice is to continuously spin the sample during data collection. A much less developed approach is to use high-energy, highly penetrating laboratory X-rays.

Another important issue in the QPA of mixtures is the limit of detection (LoD) and the limit of quantification (LoQ). In this context, the LoD can be defined as the minimal concentration of analyte that can be detected with acceptable reliability (Zevin & Kimmel, 1995), *i.e.* for which its strongest (not overlapped) diffraction peak in the powder pattern has a signal-to-noise ratio larger than 3.0. The 'reliability' criterion is flexible and may be defined by regulatory agencies, as is mainly the case for active pharmaceutical ingredients. Evidently, the LoD can be reduced (improved) by increasing the intensity of the X-ray source, for example using synchrotron radiation. In this context, the LoQ

can be defined as the minimum content of an analyte that can be determined with a value at least three times larger than its standard deviation and determined to an acceptable reliability level. For RQPA, this type of approach can be straightforward, although the accuracy for minor phases may be quite poor.

The main aim of the study described here was to test whether the use of high-energy Mo radiation, combined with high-resolution X-ray optics, could yield more accurate RQPA than well established procedures using Cu radiation. In order to do so, three sets of mixtures with increasing amounts of a given phase (the spiking method) were prepared and the corresponding RQPA results were evaluated with calibration curves (least-squares fits) and quantitatively by statistical analysis based on the Kullback–Leibler distance (KLD; Kullback, 1968). The three series were (i) crystalline inorganic phase mixtures with increasing amounts of an inorganic phase, (ii) crystalline organic phase mixtures with increasing amounts of an organic compound and (iii) a series with an increasing content of amorphous ground glass. This last series is the most challenging case because the amorphous content is derived from a small overestimation of the internal standard employed. Amorphous content determination is important for many industries, including cements, glasses, pharmaceuticals and alloys.

### 3.10.2. Compounds and series

#### 3.10.2.1. Single phases

Table 3.10.1 provides information about the phases used in this work. Further details can be found in the original publication (León-Reina *et al.*, 2016). All of the mixtures were prepared by grinding the weighed phases by hand in an agate pestle and mortar for 20 min to ensure homogeneity.

#### 3.10.2.2. Crystalline inorganic series

A constant matrix of calcite (C), gypsum (Gp) and quartz (Q) was prepared. Six samples with known increasing amounts of insoluble anhydrite (i-A) were then produced and were labelled CGpQ<sub>x</sub>A, where *x* represents the target i-A content: 0.00, 0.125, 0.25, 0.50, 1.0, 2.0 or 4.0 wt%.

#### 3.10.2.3. Crystalline organic series

A constant matrix of glucose (G), fructose (F) and lactose (L) was prepared. Six samples with known increasing amounts of xylose (X) were then produced and labelled GFL<sub>x</sub>X, where *x* represents the target X content: 0.00, 0.125, 0.25, 0.50, 1.0, 2.0 or 4.0 wt%.

### 3. METHODOLOGY

#### 3.10.2.4. Variable amorphous content series

A constant matrix of calcite (C) and zincite (Z) was prepared. Five samples with increasing contents of amorphous ground glass (Gl) were then prepared. The elemental composition of the ground glass is given in García-Maté *et al.* (2014). The mixtures were labelled CZQ\_xGl, where  $x$  indicates 0, 2, 4, 8, 16 or 32 wt% Gl. The amorphous content was determined by adding ~20 wt% quartz (Q) as an internal standard.

#### 3.10.3. Analytical techniques

All phases and mixtures were studied with Mo  $K\alpha_1$  (transmission geometry) and Cu  $K\alpha_1$  (reflection geometry) monochromatic radiation. Table 3.10.1 shows the X-ray linear absorption coefficients for all of the phases, as microabsorption is always a concern in ROPA. A microabsorption correction was not applied in this work, but readers must be aware that this effect, if relevant, is one of the greatest source of inaccuracy in ROPA (Madsen *et al.*, 2001; Scarlett *et al.*, 2002). All of the phases were also characterized by scanning electron microscopy (see Fig. 3.10.2).

##### 3.10.3.1. Mo $K\alpha_1$ laboratory X-ray powder diffraction (LXRPD)

Mo  $K\alpha_1$  powder patterns were collected in transmission geometry in constant irradiated volume mode, in order to avoid any correction of the measured intensities, on a D8 ADVANCE (Bruker AXS) diffractometer (188.5 mm radius) equipped with a Ge(111) primary monochromator, which gives monochromatic Mo radiation ( $\lambda = 0.7093 \text{ \AA}$ ). The X-ray tube operated at 50 kV and 50 mA. The optics configuration was a fixed divergence slit ( $2^\circ$ ) and a fixed diffracted anti-scatter slit ( $9^\circ$ ). A LYNXEYE XE 500  $\mu\text{m}$  energy-dispersive linear detector, optimized for high-energy radiation, was used with the maximum opening angle. Using these conditions, the samples were measured between  $3$  and  $35^\circ 2\theta$  with a step size of  $0.006^\circ$  and with a total measurement time of 3 h 5 min. The flat samples were placed into cylindrical holders between two Kapton foils (Cuesta *et al.*, 2015) and rotated at a rate of 10 revolutions per minute during data collection. Moreover, the absorption factor of each sample was experimentally measured by comparing the direct beam with and without the sample (Cuesta *et al.*, 2015). The amount of sample loaded (which determines the height of the cylinder) in the holders was adjusted to obtain a total absorption ( $\mu t$ ) of ~1, which corresponds to an absorption factor of ~2.7 or 63% of direct-beam attenuation. For the organic samples this criterion was not followed as it would lead to very thick specimens. In this case, the maximum holder thickness was used (1.7 mm).

##### 3.10.3.2. Cu $K\alpha_1$ laboratory X-ray powder diffraction (LXRPD)

Cu  $K\alpha_1$  powder patterns for exactly the same samples were recorded in reflection geometry ( $\theta/2\theta$ ) on a X'Pert MPD PRO (PANalytical B.V.) diffractometer (240 mm radius) equipped with a Ge(111) primary monochromator, which gives monochromatic Cu radiation ( $\lambda = 1.54059 \text{ \AA}$ ). The X-ray tube was operated at 45 kV and 40 mA. The optics configuration was a fixed divergence slit ( $0.5^\circ$ ), a fixed incident anti-scatter slit ( $1^\circ$ ), a fixed diffracted anti-scatter slit ( $0.5^\circ$ ) and an X'Celerator RTMS (real-time multiple strip) detector operating in scanning mode with the maximum active length. Using these conditions, the samples were measured between  $6.5$  and  $81.5^\circ 2\theta$  with a step size of  $0.0167^\circ$  and a total measurement time of 2 h 36 min. The flat samples were prepared by rear charge of a flat sample holder in order to

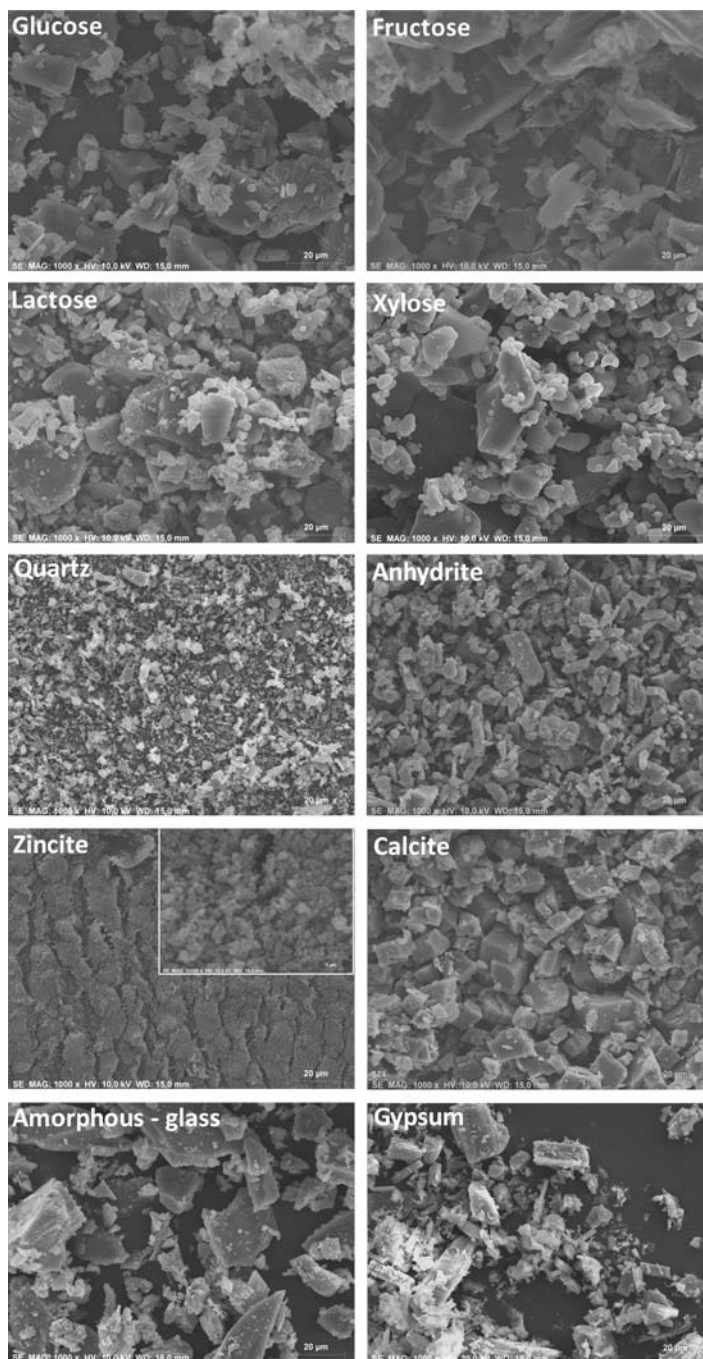


**Figure 3.10.2**

Scanning electron microscopy micrographs for the studied phases ( $\times 1000$ ). The inset in the zincite micrograph shows the powder at higher magnification ( $\times 20\,000$ ).

minimize preferred orientation and were rotated at a rate of 10 revolutions per minute.

The lowest analyte content samples, CGpQ\_0.12A and GFL\_0.12X, were measured three times using both radiations, Mo  $K\alpha_1$  and Cu  $K\alpha_1$ , for a precision (reproducibility) assessment. Therefore, regrinding and reloading of the mixtures in the sample holder was carried out prior to every measurement.

##### 3.10.3.3. Transmission synchrotron X-ray powder diffraction (SXRPD)

Powder patterns for the lowest analyte content samples, CGpQ\_0.12A and GFL\_0.12X, were also measured using synchrotron radiation. SXRPD data were collected in Debye-Scherrer (transmission) mode using the powder diffractometer at